Multivariate Identification of Extruded PLA Samples from the Infrared Spectrum

Jordi-Roger Riba (orcid: 0000-0001-8774-2389)[1], Rosa Cantero (orcid: 0000-0002-0914-9675)[2], Violeta García-Masabet(orcid: 0000-0002-5362-2896)[3], Jonathan Cailloux(orcid: 0000-0003-3785-0829)[3], Trini Canals(orcid: 0000-xxxxxxxxxxxx)[2], Maria Lluïsa Maspoch(orcid: 0000-0002-4813-6412)[3].*

*Corresponding Author: riba@ee.upc.edu

[1]Universitat Politècnica de Catalunya Tech, 08222 Terrassa (Barcelona), Spain

[2]Universitat de Lleida, 08700 Igualada (Barcelona), Spain

[3]Centre Català del Plàstic, Universitat Politècnica de Catalunya Barcelona Tech (UPC-EEBE), C/Colom 114, 08222 Terrassa, Spain

ABSTRACT

Polylactid acid (PLA) is a biodegradable thermoplastic polymer that is presented as a good alternative to petroleum-derived plastics. Some of the major drawbacks of this material are its lack of thermal stability and rapid degradation in large-scale production, thus a special care must be put in the manufacturing processes involved. To improve their properties, a reactive extrusion with a multi-epoxy chain extender (SAmfE) has been performed at pilot plant scale. The induced topological modifications produce a mixture of several types of non-uniform structures. Conventional chromatographic (SEC-static light scattering) or spectroscopic (NMR-nuclear magnetic resonance) techniques usually fail in characterizing non-uniform structures. A method for the classification of modified PLA samples based on a multivariate treatment of the spectral data obtained by Fourier-transform infrared spectroscopy (FTIR) spectroscopy, jointly with the application of feature extraction and classification algorithms, has been applied in this study. The

results of this work show the potential of the methodology proposed as a fast tool for process control.

Keywords – process control; infrared spectroscopy; polylactid acid; classification.

1. INTRODUCTION

One of the key bio-based polymers to substitute petroleum-based polymers in common applications is Poly(lactic acid) (PLA) [1]. PLA is a polyester, specifically a linear aliphatic thermoplastic. It is obtained by ring-opening polymerization of lactide, whose lactic acid monomers are usually produced by fermenting sugar feed stocks [2].

PLA has several applications in different sectors, including film and packaging, textile and fibers, or construction and automotive products [2, 3]. Moreover, due to its non-toxic characteristics, biodegradability and biocompatibility, PLA is often considered for biomedical applications, in areas such as tissue engineering, drug delivery, blood vessel, scaffolding [4] or temporary implants [5].

Regardless of its prominent properties some difficulties had to be dealt with for PLA to properly occupy a position as a commodity plastic, along with the advantages of been a biosourced one.

Some of the drawbacks of PLA can affect directly the kind of processing available, particularly the polyester nature of PLA will require a special processing due to its thermal stability and rapid degradation that difficult its manufacturing and application in large-scale productions. Likewise, PLA can have a low melt strength that could reduce the available processes to use, like extrusion blowing or deep thermoconforming. These drawbacks had led to several approaches and numerous studies in order to improve PLA behavior [3, 6–8].

Therefore, reactive extrusion in combination with a multifunctional reactive agent, is considered as a promising method for enhancing and stabilizing melt PLA properties [3, 6]. Among the most frequently applied chain extenders, the different reactives which are able to react with PLA functional end groups -OH and -COOH are, isocyanate [8], epoxy [7], isocyanurate and anhydride [9] functions. Among the most common reactive agents used as chain extenders in PLA, it can be found SAmfE (Joncryl®), this epoxy multifunctional reactive can develop chemical bonding of several PLA chains. The topological modifications induced with the reactive agent produce a mixture of diverse types of non-uniform structures with different architectures and molecular weights, due to the possible competition between chain degradation, chain extension, and chain branching [9].

Unfortunately, there is a lack of characterization methods to evaluate the modification of the PLA with the reactive agent in a molecular level due to a limited sensibility to highlight the non-uniform changes with conventional techniques as Nuclear Magnetic Resonance Spectroscopy (NMR) or Chromatography like SEC-static light scattering (SEC-LS). On this basis, an indirect method has been used to evaluate a final property like viscosity to assess the performance of the reactive agent and develop a method to control the structural modification at large scale processing. However, the control of the process is difficult, not only the reactions are random but the processing require a continuous system where the control is mainly in the feed stage of the extrusion to produce the desired outcome, the reaction inside the equipment only can be controlled with the content of the reactive in the feed and subsequently the characterization of the output of the process that has been established that can be problematical [10].

A characterization technique like Fourier Transform Infrared spectroscopy (FTIR) has been used to evaluate the possible reactions with the chain extender without success due to the few

content of covalent bonding produce in the reaction to be around the detection limit of the technique. FTIR is a nondestructive instrumental technique that allows extracting the chemically relevant information contained in every sample [11]. It is known that the joint use of a limited amount of experimental data and suitable mathematical models, it is possible to predict with reliability some key properties of the chemical samples analyzed [12]. However, a multivariable mathematical method using a computing analysis of principal components (PCA) in FTIR together with canonical variables (CVA) has been successfully applied to evidence possible coupling reactions between PLA functional end groups and the epoxy groups of the SAmfE. As a result of the limited alternative to directly evaluate the relationship between structural changes and the concentration of additive use, the aim of this work is to evaluate the applicability of the PCA-CVA multivariable methods coupled to FTIR to highpoint the concentrations applied in the polymer modified through reactive extrusion in a pilot plant.

This paper makes different contributions in the area of PLA production, including the inherent environmental advantages of using such biodegradable polymer in front of other oil-derived polymers. First, the outcomes of this work contribute to the optimization of the percentage of chain extender (SAmfE), which plays a fundamental role on providing PLA polymer the required stability to be produced on an industrial scale. Next, the multivariate approach presented has several appealing features, including very fast response, easy application, high reliability, or the fact that it does not require treatment or destruction of the samples, with the consequent saving of contaminating reagents. Therefore, it can be applied as a possible control tool during production of PLA polymer.

2. THE SAMPLES ANALYZED

As explained, this paper performs an identification of PLA samples containing styrene-acrylic multifunctional-epoxide (SAmfE) from those that do not include this reactive agent. But even more, it identifies the concentration or percentage composition of SAmfE.

A commercial PLA extrusion grade (Ingeo PLA 4032D) was purchased from NatureWorks and used as received. SAmfE reactive agent, namely Joncryl® ADR-4300F), was kindly supplied by BASF in flake form. It has a functionality of 12, a molecular weight of 5443 $g.mol^{-1}$ and an epoxy equivalent weight of 433 $g.mol^{-1}$.

Prior to each processing, PLA pellets were dried during 4h at 80ºC in a PIOVAN (DSN506HE) hopper-dryer (dew point =-40ºC). Initially, a PLA-based masterbatch of SAmfE was prepared using a single screw extruder (IQAP-LAP E-30/25, screw diameter: 30mm, L/D=25). The temperature profile was 120, 130, 130 and 135 ºC from the feeding zone to the die, respectively and the screw speed was fixed at 35 rpm. The extrudate was water-cooled and pelletized for further use.

Afterwards, the masterbartch pellets were diluted with neat PLA to obtain a nominal concentration of 0.5, 0.6 and 1.25 wt.% of SAmfE, respectively. These groups of materials were achieved through reactive extrusion using a co-rotating twin-screw extruder (COLLIN Kneter 25X24D, screw diameter: 25 mm, L/D = 36) with a screw speed of 35 rpm. The seven heating zone were set to 45, 165, 165, 170, 180, 190, 190 °C from the feeding zone to the die, respectively. A N_2 blanket was introduced in the hopper of the feeding zone and vacuum was applied to the metering zone.

Since SAmfE is a multi-functional reactive agent, Figure 1 shows the different reaction mechanisms that can take place between the functional end groups of PLA and the epoxy groups of SAmfE.

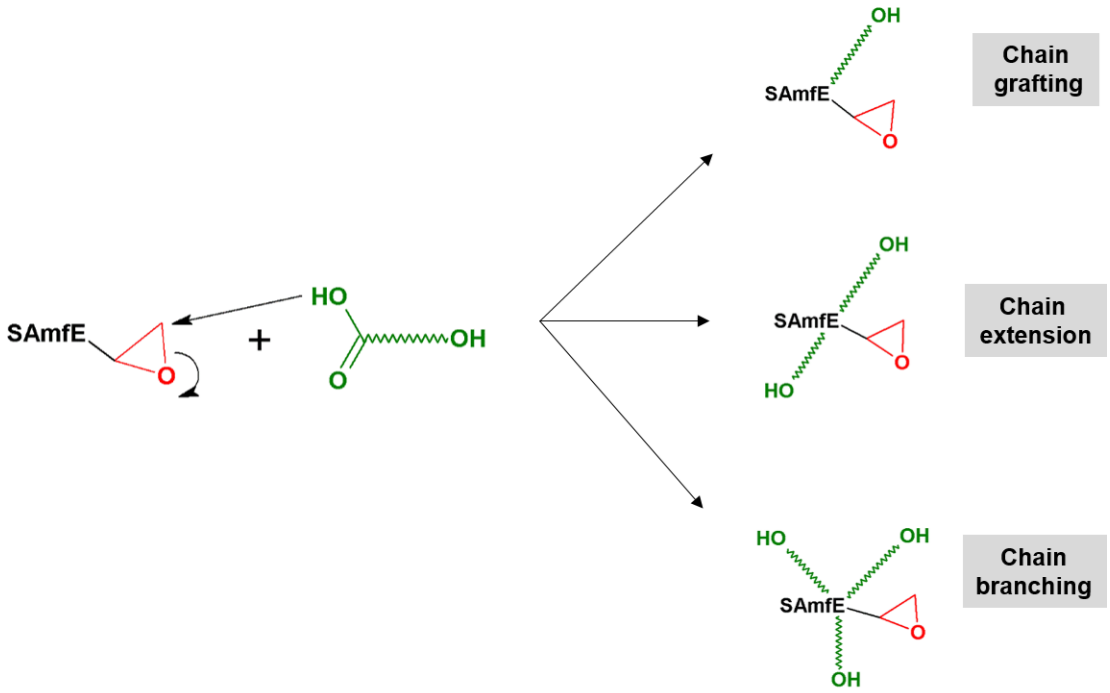

Figure 1. Proposed reaction mechanisms between PLA and SAmfE

In this paper a total of 200 PLA samples were analyzed, which contain different composition of SAmfE. The 200 PLA samples are divided in four groups of 50 samples each, namely 0%, 0.5%, 0.6% and 1.25%, respectively, according to the percentage composition of SAmfE. The reference percentage of SAmfE was calculated as the mass percentage added during the PLA manufacturing process in the pilot plant.

3. MATERIALS AND METHODS

This research has been performed at pilot plant level and is proposed to be applied as a quality control method.

As in other works [13], A PerkinElmer Spectrum One (S/N 57458, Beaconsfield, UK) ATR-FTIR spectrometer was used to acquire the reflectance spectra of the 200 analyzed PLA samples. The spectra were acquired in a controlled laboratory at 25 ± 1ºC. To reduce the noise, 4 scans per sample were taken in the 4000–650 cm^{-1} wavenumber interval, with 1 cm^{-1} resolution. Therefore, each raw spectrum includes 3351 spectral points. The first and second derivative of all spectra was performed in order to increase the performance of the multivariate statistical methods applied to identify the PLA samples with different composition.

To generate the classification model, the whole set of samples is split them into a calibration and a prediction set. Whereas the calibration set is used to calibrate the mathematical model, the prediction set is used to evaluate the performance of the mathematical model. To this end the whole body of 200 PLA samples was randomly slit into 100 calibration samples and 100 prediction samples, as detailed in Table 1.

Table 1. Number of PLA samples in each set of data

Identification groups	Calibration set	Prediction set
0% SAmfE	25	25
0.5% SAmfE	25	25
0.6% SAmfE	25	25
1.25% SAmfE	25	25

Spectral data is the input information provided to the multivariate methods to identify or classify unknown incoming samples within their pertinence group, according to their composition. Figure 2 shows the approach applied to identify the samples, which is based on the of a preprocessing of the spectral data flowed by the subsequent application of principal components analysis (PCA), canonical variate analysis (CVA) and the *k* nearest neighbor algorithm (*k*-NN), as summarized in

Figure 2. It is noted that the preprocessing stage consists calculating the first and second derivatives of the spectral data.

Since the ATR-FTIR spectra are composed of 3351 wavenumbers, there is an imperious need to apply suitable multivariate methods to reduce their dimensionality, thus retaining the analytically significant data in a reduced set of latent variables [14, 15] while minimizing the random noise included in the raw spectra.

In this paper a three-steps transformation of the original data set $X_{(n,m)}$ is performed by applying a preprocessing stage, followed by the application of PCA and CVA multivariate methods. All this mathematical process can be understood as a transformation in which the transformation matrix if found as,

$$X_{\text{transformed}(n,m^{**})} = X_{(n,m)} \cdot V_{total(m,m^{**})} \quad (1)$$

where

$$V_{total(m,m^{**})} = V_{prep(m,m)} \cdot V_{PCA(m,m^{*})} \cdot V_{\text{CVA}(m^{*},m^{**})} \quad (2)$$

n being the number of PLA samples analyzed, m the number of wavenumbers in each spectrum, $m^* << m$ the number of latent variables provided by the PCA algorithm , also known as principal components (PCs), and $m^{**} < m^*$ the number of latent variables provided by the CVA algorithm [16, 17], the canonical variates (CVs). It is noted that CVA is closely related to the linear discriminant analysis (LDA) transformation, which foundations are found in [18, 19]. Finally, V_{prep}, V_{PCA} and V_{CVA} are the transformation matrixes found in the preprocessing, PCA and CVA stages. It is noted that both PCA [20] and CVA algorithms aim at reducing the dimensions of the problem, so $m^* << m$ and $m^{**} < m$. Further background and mathematical details about the PCA and CVA algorithms can be found in [21–23] and [24–26], respectively.

Finally, to identify in which group an unknown sample of the prediction set belongs, the *k*-NN classifier algorithm [27–29] is applied to the transformed data matrix $X_{\text{pre,transformed}(n,m^{**})}$. It is worth noting that this mathematical method provides as many output values as classes or groups have been defined, four in this case. These output values are normalized in within 0-1, this value quantifying the membership degree of the sample analyzed in each class.

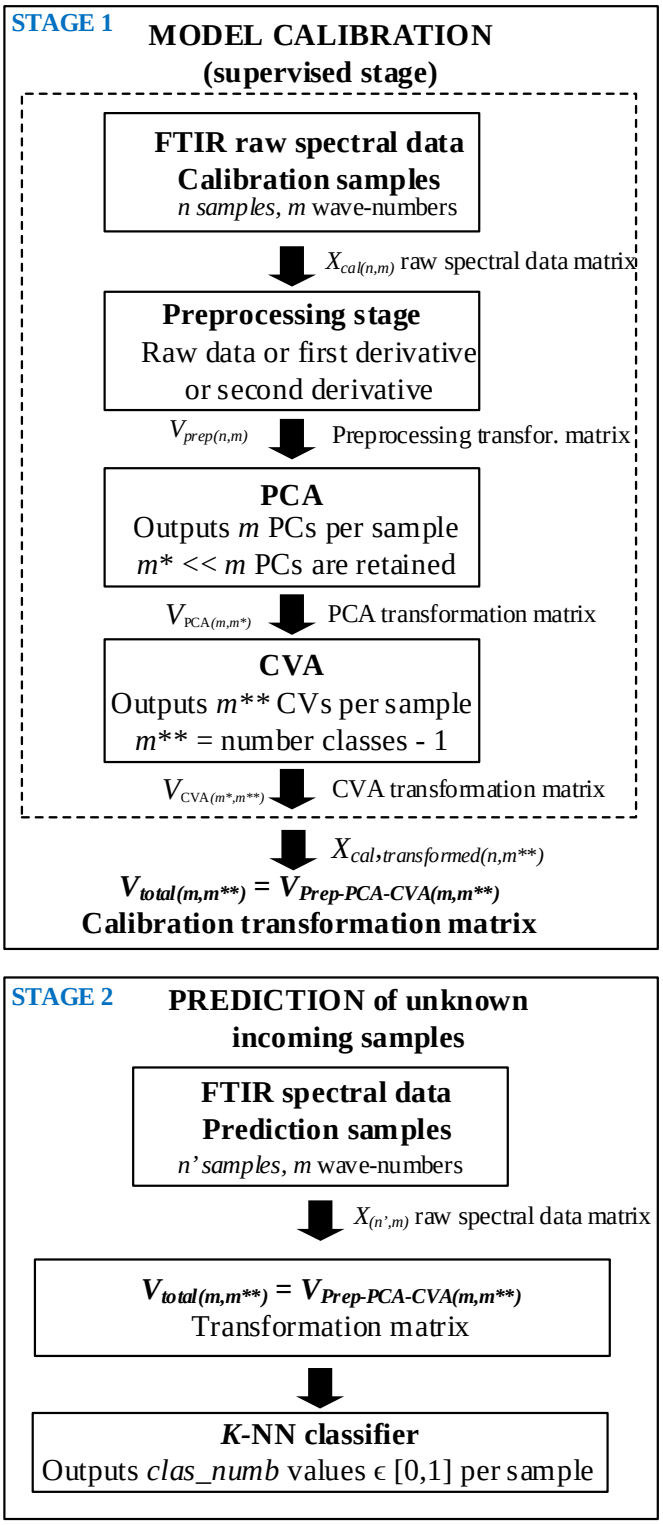

Figure 2. Flowchart of the multivariate approach proposed in this paper to identify unknown incoming samples from the spectral information provided by the FTIR spectra. It is based on a preprocessing stage, followed by the subsequent application of PCA, CVA and *k*-NN.

4. RESULTS

Figure 3 shows the ATR-FTIR spectra of one sample of each group. From a simple visual inspection of such spectral data it is not possible to detect differences among the different spectral bands between the samples that do not contain the extruder agent and those containing several amounts of the same, thus corroborating the need of applying powerful multivariate mathematical tools to correctly classify unknown incoming samples in the different groups.

This work assumes that the differences among the molecular structures of the four groups of samples studied can be revealed by analyzing the data in the 3351 wavenumbers of the ATR-FTIR spectra.

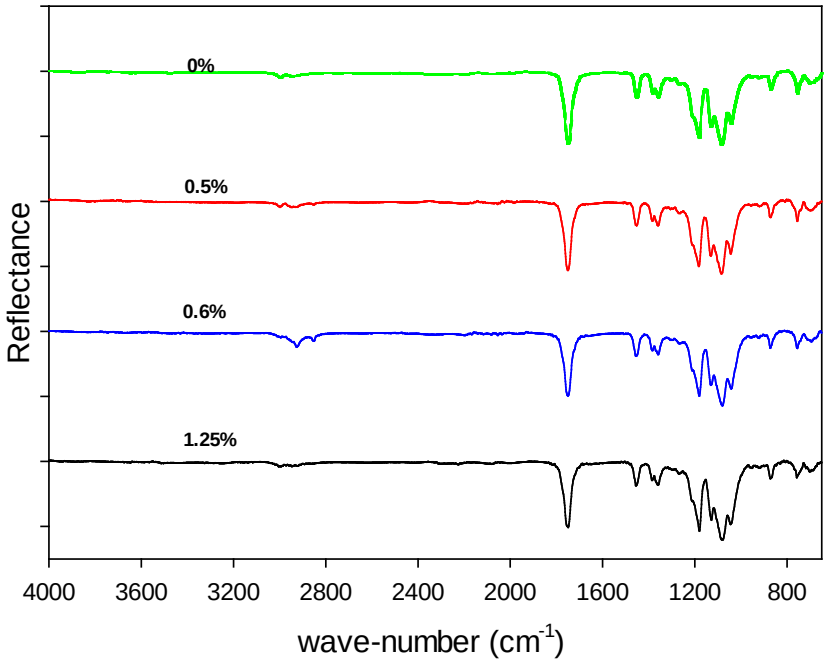

Figure 3. ATR-FTIR reflectance data of one sample of each analyzed group (0%, 0.5%, 0.6% and 1.25% SAmfE).

The characteristic band assignments for each PLA-based material are summarized in Table 2. These are the characteristic bands of PLA, so the extruder agent does not cause any significant difference in these bands.

Table 2. Wavenumbers and their corresponding vibrational assignments for PLA-based samples IR spectra [3, 30].

Wavenumbers, ν (cm^{-1})	Assignments	Nature of vibration *
756	Crystalline phase	-
871	Amorphous phase	-
868	C-C	st
1045	$C\text{-}CH_3$	st
1093, 1130, 1184	C-O-C	st as
1268	C=O	δ
1360, 1382	CH	δ (s and as)
1453	CH_3	δ as
1757	C=O	st
2880	C-H	st s
2945, 2994	$C\text{-}CH_3$	st (s and as)

* st: stretching (ν), δ: bending, s: symmetrical, as: asymmetrical

Figure 4 shows the FTIR spectrum of the extraction product SAmfE, where the characteristic bands of the styrene function are observed at 3000-3100 cm^{-1}, 2000-1800 cm^{-1} and 800-600 cm^{-1}, of the carboxylic ester, ester and alkyl groups described in Table 2. In addition, Figure 4 shows another band or multiple signal near 1250 cm^{-1}, which is characteristic of the epoxy function.

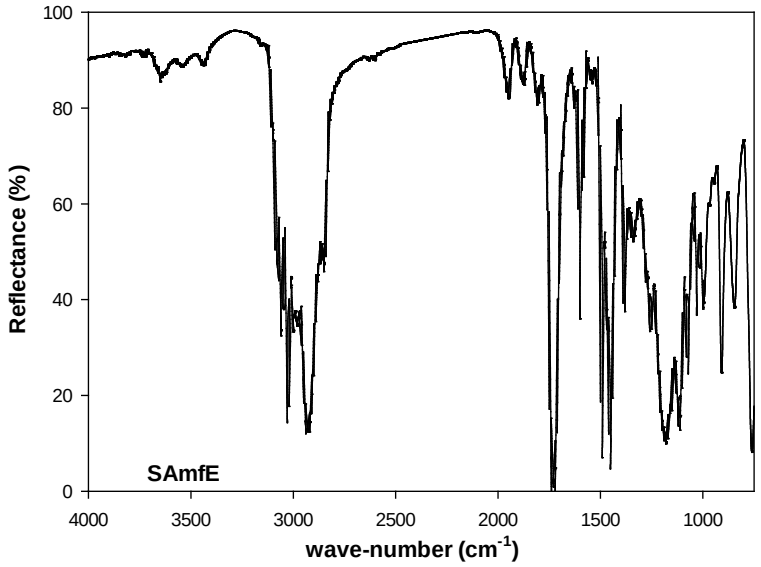

Figure 4. ATR-FTIR spectrum of the chain extender SAmfE.

The ATR-FTIR spectra of the studied samples presented in Figure 3 almost do not allow to observe the characteristic signal of the described epoxy group, nor in the form of the spectral bands nor in the intensity of the same.

PLA samples are classified based on the information extracted from the ATR-FTIR spectra. Therefore, the strategy summarized in the flowchart shown in Figure 2. Therefore, the preprocessing (first and second derivative of the reflectance spectra), PCA and CVA algorithms are sequentially applied to the samples in the calibration set to build or calibrate the mathematical model. Next, with the samples in the prediction set are identified from the transformation matrix obtained in the calibration stage and by applying the *k*-NN algorithm.

Next sections show the identification results attained taking into account the raw spectral ATR-FTIR data, and the first and second derivatives of the spectra.

4.1 First study analyzing 200 samples of four groups (0%, 0.5%. 0.6% and 1.25%)

In this study the 200 PLA samples with different content of SAmfE are analyzed. As explained, 100 samples randomly selected were assigned to the calibration set, whereas the remaining 100

samples were assigned to the prediction set. The elements in each group are detailed in Table 1. The aim of this study is to correctly identify the 100 samples in the calibration set from the ATR-FTIR spectral data.

Since raw spectra include the reflectance values corresponding to 3351 wavenumbers, the different matrixes dealt with in this work are summarized in Table 3.

Table 3. Raw ATR-FTIR data matrixes of the 200 PLA samples analyzed

Identification groups	Calibration set	Prediction set
0% SAmfE	$X_{cal,0\%(25,3351)}$	$X_{pre,0\%(25,3351)}$
0.5% SAmfE	$X_{cal,0.5\%(25,3351)}$	$X_{pre,0.5\%(25,3351)}$
0.6% SAmfE	$X_{cal,0.6\%(25,3351)}$	$X_{pre,0.6\%(25,3351)}$
1.25% SAmfE	$X_{cal,1.25\%(25,3351)}$	$X_{pre,1.25\%(25,3351)}$

The n rows of $X_{(n,m)}$ correspond to the different samples, whereas the m columns correspond to the reluctance value of each wavenumber. The raw spectral data matrix $X_{cal(n,m)}$ includes n = 100 calibration samples and m = 3351 wavenumbers. The PCA outputs the same number of PCs as wavenumbers, that is, 3351 PCs. However, in order to boost the discrimination among groups, only the first ranked PCs explaining 99.9% of the overall variance are retained. It usually implies a great dimensionality reduction, which is required for a subsequent application of the CVA algorithm.

In this section three studies were carried out, with the raw ATR-FTIR spectral data and the first and second derivative of the raw spectra, respectively.

Figure 5 shows the results attained from the raw spectral data when retaining the first 46 PCs (99.9% of variance), which lead to a success rate in identifying prediction samples between 92 and 94%, as summarized in Table 4.

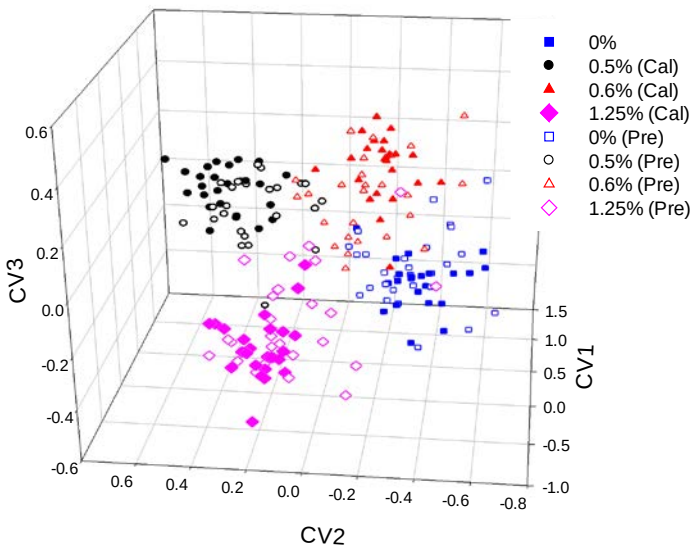

Figure 5. Identification results from the raw ATR-FTIR spectra. Calibration and prediction PLA samples plotted in the space defined by the three CVs calculated from the CVA algorithm, previous application of the PCA algorithm.

Next, the same strategy was applied from the first derivative of the spectral data. Figure 6 shows the results attained from the raw spectral data when retaining the first 73 PCs (99.9% of variance), which lead to a success rate in identifying prediction samples between 88 and 90%, as shown in Table 4.

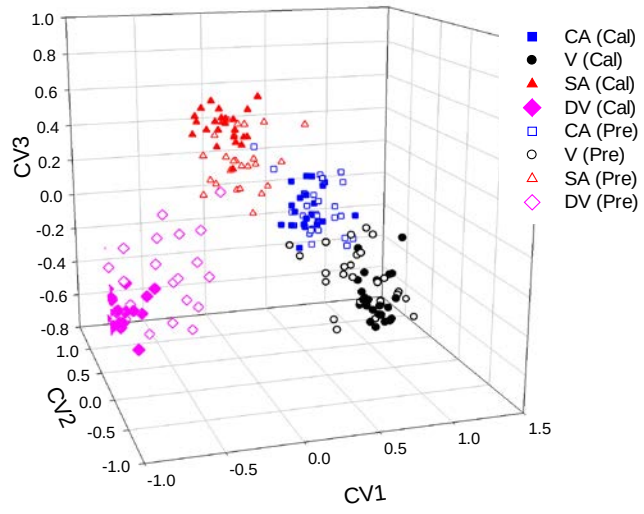

Figure 6. Identification results from the first derivative of the ATR-FTIR spectra. Calibration and prediction PLA samples plotted in the space defined by the three CVs calculated from the CVA algorithm, previous application of the PCA algorithm.

Finally, the performance of the second derivative of the spectral data was studied. Figure 7 shows the results attained from the raw spectral data when retaining the first 73 PCs (99.9% of variance), which lead to a success rate in identifying prediction samples between 91 and 92%, as shown in Table 4.

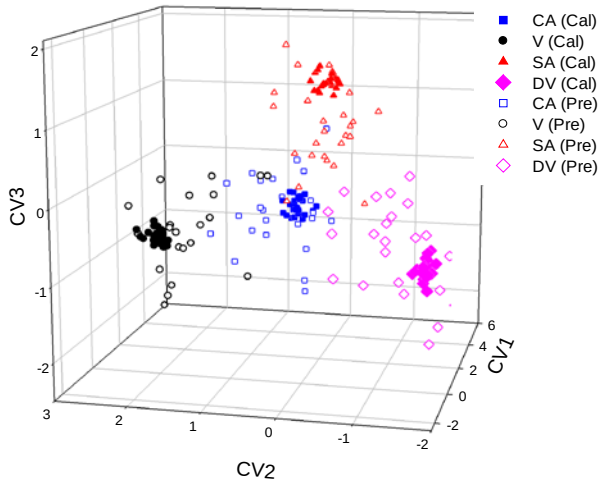

Figure 7. Identification results from the second derivative of the ATR-FTIR spectra. Calibration and prediction PLA samples plotted in the space defined by the three CVs calculated from the CVA algorithm, previous application of the PCA algorithm.

Table 4. Identification success rate following the preprocessing + PCA + CVA + *k*-NN approach (200 PLA samples of groups 0%, 0.5%, 0.6% and 1.25% SAmfE)

Preprocessing	$k = 3$	$k = 4$	$k = 5$	$k = 6$
Raw spectral data	92/100	93/100	93/100	94/100
First derivative	88/100	89/100	90/100	90/100

Second derivative	91/100	92/100	92/100	92/100

4.2 Second study analyzing 100 samples of two similar groups (0.5% and 0.6%)

Previous studies show that the manufactured material achieves the best properties when the concentration of SAmfE is approximately 0.5% [9]. In order to focus special attention on this range of concentrations, a second study is carried out. In this second study the discrimination power of proposed approach is tested by only analyzing the samples in the 0.5% and 0.6% groups, since these samples have very similar compositions. Therefore this is a challenging problem.

In this study 100 PLA samples of with 0.5% and 0.6% of SAmfE are analyzed. As before, 50 samples were randomly assigned to the calibration set, whereas the remaining 50 samples were assigned to the prediction set. The elements in each group are detailed in Table 5.

Table 5. Raw data ATR-FTIR matrixes

Identification groups	Calibration set	Prediction set
0.5% SAmfE	$X_{cal,0.5\%(25,3351)}$	$X_{pre,0.5\%(25,3351)}$
0.6% SAmfE	$X_{cal,0.6\%(25,3351)}$	$X_{pre,0.6\%(25,3351)}$

This section performs three studies. The first one considers the raw ATR-FTIR spectral data, whereas the second and third studies consider the first and second derivative of the raw spectral data, respectively.

Figure 8 shows the results attained from the raw spectral data when retaining the first 31 PCs (99.9% of variance), which lead to a success rate in identifying prediction samples of 98%, as summarized in Table 6.

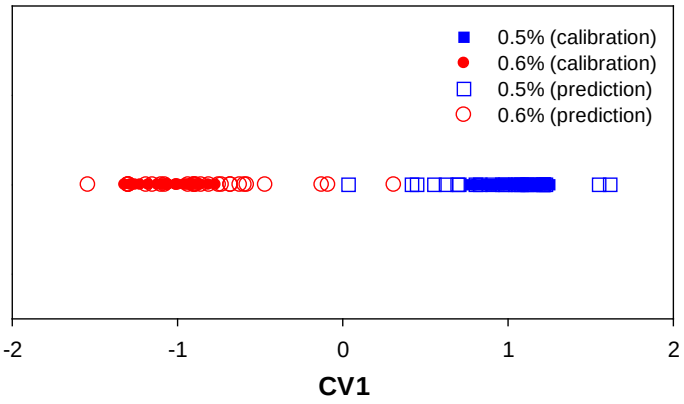

Figure 8. Identification results from the raw ATR-FTIR spectra. Calibration and prediction PLA samples plotted in the space defined by the unique CV calculated from the CVA algorithm, previous application of the PCA algorithm.

Next, the same strategy was applied from the first derivative of the spectral data. Figure 9 shows the results attained from the raw spectral data when retaining the first 48 PCs (99.9% of variance), which lead to a success rate of 100% in identifying the 50 prediction samples, as shown in Table 6.

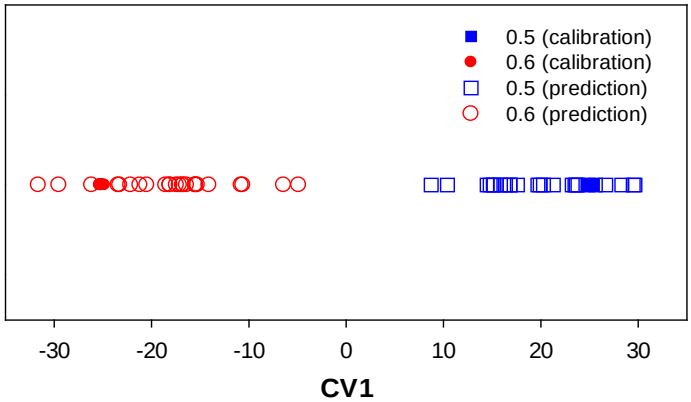

Figure 9. Identification results from the first derivative of the ATR-FTIR spectra. Calibration and prediction PLA samples plotted in the space defined by the unique CV calculated from the CVA algorithm, previous application of the PCA algorithm.

Finally, the performance of the second derivative of the spectral data was studied. Figure 10 shows the results attained from the raw spectral data when retaining the first 44 PCs (99.9% of variance), which lead to 100% success rate in identifying the 50 prediction samples, as shown in Table 6.

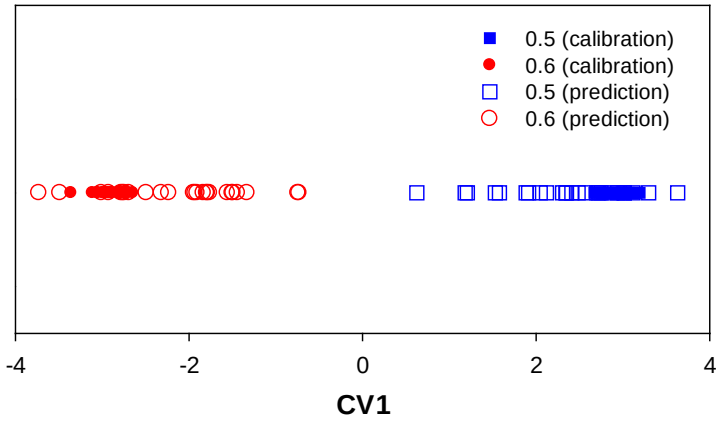

Figure 10. Identification results from the second derivative of the ATR-FTIR spectra. Calibration and prediction PLA samples plotted in the space defined by the unique CV calculated from the CVA algorithm, previous application of the PCA algorithm.

Table 6 summarizes the results attained with the PCA + CVA + *k*-NN approach from the raw spectral data, and the first- and second-derivate of the spectra.

Table 6. Identification success rate following the preprocessing + PCA + CVA + *k*-NN approach (100 PLA samples of groups 0.5% and 0.6%)

Preprocessing	$k = 3$	$k = 4$	$k = 5$	$k = 6$
Raw spectral data	49/50	49/50	49/50	49/50
First derivative	50/50	50/50	50/50	50/50
Second derivative	50/50	50/50	50/50	50/50

Results shown in Table 6 prove the accuracy and reliability of the proposed approach, since the identification success rate is close to 100% for all samples analyzed.

5. CONCLUSIONS

In this study, PLA linear topology was modified through reactive extrusion using a multi-functional reactive agent. The different controls carried out in the manufactured product only allow to compare the properties obtained according to the proportions of the reagent added to extrude the polymer.

In this paper, a non-invasive, non-destructive, fast and easy-to-apply method to determine the amount of SAmfE reagent added has been proposed. It is based on a multivariate chemometric treatment of FTIR spectral data through the PCA + CVA algorithms and the *k*-NN classifier.

Results reported in this paper have shown the suitability and applicability of this method since success rates in classifying unknown incoming PLA samples, 94% in the first study (4 groups) and can be as high as 100% in the second study (2 groups) in spite of the little difference of concentration of extruder agent in both groups.

ACKNOWLEDGEMENTS

The authors acknowledge the financial support from the Spanish Ministry of Economy and Competitiveness through the project MAT2016-80045-R (AEI/FEDER, UE).

REFERENCES

1. Cailloux J, Abt T, Garcia-Masabet V, et al (2018) Effect of the viscosity ratio on the PLA/PA10.10 bioblends morphology and mechanical properties. express Polym Lett 12:569–582. https://doi.org/10.3144/expresspolymlett.2018.47

2. Lunt J (1998) Large-scale production, properties and commercial applications of polylactic acid polymers. Polym Degrad Stab 59:145–152. https://doi.org/10.1016/S0141-3910(97)00148-1

3. Garlotta D (2001) A Literature Review of Poly(Lactic Acid). J Polym Environ 9:63–84.

https://doi.org/10.1023/A:1020200822435

4. Nofar M, Sacligil D, Carreau PJ, et al (2019) Poly (lactic acid) blends: Processing, properties and applications. Int J Biol Macromol 125:307–360. https://doi.org/10.1016/J.IJBIOMAC.2018.12.002

5. Chu C, Li X, Yu W, et al (2019) Degradation behaviors of PLA-matrix composite with 20 vol% magnesium alloy wires under static loading conditions. J Mater Sci 54:4701–4709. https://doi.org/10.1007/s10853-018-03199-5

6. Auras R, Harte B, Selke S (2004) An Overview of Polylactides as Packaging Materials. Macromol Biosci 4:835–864. https://doi.org/10.1002/mabi.200400043

7. Anderson K, Schreck K, Hillmyer M (2008) Toughening Polylactide. Polym Rev 48:85–108. https://doi.org/10.1080/15583720701834216

8. Liu H, Zhang J (2011) Research progress in toughening modification of poly(lactic acid). J Polym Sci Part B Polym Phys 49:1051–1083. https://doi.org/10.1002/polb.22283

9. Cailloux J, Santana OO, Franco-Urquiza E, et al (2014) Sheets of branched poly(lactic acid) obtained by one-step reactive extrusion–calendering process: physical aging and fracture behavior. J Mater Sci 49:4093–4107. https://doi.org/10.1007/s10853-014-8101-y

10. Cailloux J, Santana OO, Maspoch ML, et al (2015) Using viscoelastic properties to quantitatively estimate the amount of modified poly(lactic acid) chains through reactive extrusion. J Rheol (N Y N Y) 59:1191–1227. https://doi.org/10.1122/1.4928071

11. Dou T, Jing N, Zhou B, Zhang P (2018) In vitro mineralization kinetics of poly(l-lactic acid)/hydroxyapatite nanocomposite material by attenuated total reflection Fourier

transform infrared mapping coupled with principal component analysis. J Mater Sci 53:8009–8019. https://doi.org/10.1007/s10853-018-2169-8

12. Pilania G, Liu X-Y, Wang Z (2019) Data-enabled structure–property mappings for lanthanide-activated inorganic scintillators. J Mater Sci 54:8361–8380. https://doi.org/10.1007/s10853-019-03434-7

13. Jiang Y, Zhang SY, Zhang XL, Zhang T (2018) Improving the performance of UV-curable coatings with carbon nanomaterials. express Polym Lett 12:628–639. https://doi.org/10.3144/expresspolymlett.2018.53

14. Hernández-Guiteras J, Riba J-R, Romeral L (2014) Redesign process of a 765kVRMS AC substation connector by means of 3D-FEM simulations. Simul Model Pract Theory 42:1–11. https://doi.org/10.1016/j.simpat.2013.12.001

15. Riba JR, Cailloux J, Cantero R, et al (2018) Multivariable methods applied to FTIR: A powerful technique to highlight architectural changes in poly(lactic acid). Polym Test 65:. https://doi.org/10.1016/j.polymertesting.2017.12.003

16. Jiang B, Zhu X, Huang D, et al (2015) A combined canonical variate analysis and Fisher discriminant analysis (CVA–FDA) approach for fault diagnosis. Comput Chem Eng 77:1–9. https://doi.org/10.1016/J.COMPCHEMENG.2015.03.001

17. Lu Q, Jiang B, Gopaluni RB, et al (2018) Locality preserving discriminative canonical variate analysis for fault diagnosis. Comput Chem Eng 117:309–319. https://doi.org/10.1016/J.COMPCHEMENG.2018.06.017

18. Zhang Y, Zhang N, You D, et al (2019) High-power disk laser welding statuses monitoring

based on analyses of multiple-sensor signals. J Manuf Process 41:221–230. https://doi.org/10.1016/J.JMAPRO.2019.03.028

19. Liu J, Hu Y, Wu B, Wang Y (2018) An improved fault diagnosis approach for FDM process with acoustic emission. J Manuf Process 35:570–579. https://doi.org/10.1016/J.JMAPRO.2018.08.038

20. Zhang Z, Zhang L, Wen G (2019) Study of inner porosity detection for Al-Mg alloy in arc welding through on-line optical spectroscopy: Correlation and feature reduction. J Manuf Process 39:79–92. https://doi.org/10.1016/J.JMAPRO.2019.02.016

21. Maurya D, Tangirala AK, Narasimhan S (2018) Identification of Errors-in-Variables Models Using Dynamic Iterative Principal Component Analysis. Ind Eng Chem Res 57:11939–11954. https://doi.org/10.1021/acs.iecr.8b01374

22. Luo L, Bao S, Tong C (2019) Sparse Robust Principal Component Analysis with Applications to Fault Detection and Diagnosis. Ind Eng Chem Res 58:1300–1309. https://doi.org/10.1021/acs.iecr.8b04655

23. R. A. Johnson, Wichern DW (2007) Applied Multivariate Statistical Analysis, 6th editio. Prentice-Hall, Englewood Cliffs, NJ (USA)

24. Riba J-R, Canals T, Cantero R, Iturriaga H (2011) Potential of infrared spectroscopy in combination with extended canonical variate analysis for identifying different paper types. Meas Sci Technol 22:025601. https://doi.org/10.1088/0957-0233/22/2/025601

25. Nørgaard L, Bro R, Westad F, Engelsen SB (2006) A modification of canonical variates analysis to handle highly collinear multivariate data. J Chemom 20:425–435.

https://doi.org/10.1002/cem.1017

26. Capelli F, Riba J-R, Rodriguez A, Lalaouna S (2017) Research Towards Energy-Efficient Substation Connectors. Springer International Publishing, pp 295–301

27. Riba J-R, Canals T, Gómez R (2012) Comparative Study of Multivariate Methods to Identify Paper Finishes Using Infrared Spectroscopy. IEEE Trans Instrum Meas 61:1029–1036. https://doi.org/10.1109/TIM.2011.2173048

28. Taqvi SA, Tufa LD, Zabiri H, et al (2018) Multiple Fault Diagnosis in Distillation Column Using Multikernel Support Vector Machine. Ind Eng Chem Res 57:14689–14706. https://doi.org/10.1021/acs.iecr.8b03360

29. Yuan S, Jiao Z, Quddus N, et al (2019) Developing Quantitative Structure–Property Relationship Models To Predict the Upper Flammability Limit Using Machine Learning. Ind Eng Chem Res acs.iecr.8b05938. https://doi.org/10.1021/acs.iecr.8b05938

30. Gonçalves CMB, Coutinho JAP, Marrucho IM (2010) Optical Properties. In: Poly(Lactic Acid). John Wiley & Sons, Inc., Hoboken, NJ, USA, pp 97–112